MODELLING THE THERMAL AND COMPOSITIONAL EVOLUTION OF ICY SATELLITES, WITH APPLICATION TO PLUTO AND TRITON. J.W. Miller[1,2] (juliawmiller@g.ucla.edu), S.M. Howell[2], and E. Lesage[2]. [1]Department of Earth, Planetary, and Space Sciences, University of California, Los Angeles, Los Angeles, CA, USA, 90095. [2]Jet Propulsion Laboratory, California Institute of Technology, Pasadena, CA, USA, 91109.

Introduction: Triton and Pluto share similarities in size, bulk density, surface temperature, and likely origins[1,2]. Still, significant differences between the spectra of Pluto and Triton were noted using ground-based telescopes[3], and the New Horizons flyby of Pluto in 2015 revealed a largely unique body in terms of both surface morphology and the inventory and distribution of volatile species[4,5,6,7].

Differences in surface composition may be indicative of different formation environments or timescales, but the lack of constraints on these parameters within the Kuiper belt makes the likelihood of this possibility difficult to evaluate. The aim of this study is to create a numerical model which can be used to determine whether differences in internal heating driven by capture and tidal forces might account for the morphological and compositional differences between the surfaces of Pluto and Triton.

Complex and computationally expensive 3-dimensional problems can be greatly simplified by assuming radial symmetry, negating variations about the zenith and azimuthal directions. Numerous such 1-dimensional models of 3-dimensional targets have been developed to explore various aspects of icy body interiors: Tobie et al. (2005) consider the effects of tidal dissipation and ammonia concentration on the evolution of Titan's interior structure, while Desch et al. (2009) focus on the significance of ammonia for initiating differentiation in KBOs. Models for the evolution of water ice shells have been developed by Robuchon and Nimmo (2011) and Nimmo and Spencer (2015) for Pluto and Triton respectively.

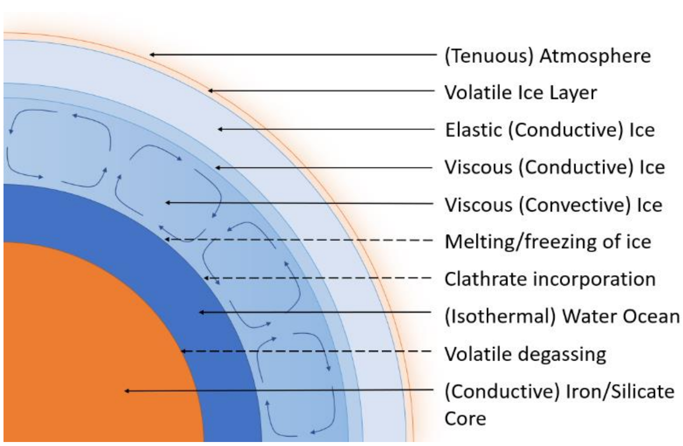

Figure 1: Model schematic showing the different layers (solid arrows) and processes (dashed arrows) considered. Layer thicknesses are not to scale.

More detailed compositional models for icy bodies have been created in recent years[12,13], but limitations in computational power and time mean that such models are best suited for systems in or near equilibrium.

We are building on the ideas explored in these studies by developing a model framework for the self-consistent, energetically conservative thermal and compositional evolution of an icy body on billion-year timescales. We focus on the treatment of independently evolving orbital parameters and an ice shell which includes multiple volatile species.

Model Description: We present an explicit forward-in-time finite element model with spherical symmetry and a pseudo-Lagrangian reference frame. The model is still in development but has been designed to be as simple as possible, abstracting complex behavior through first-principles physical descriptions, while including the key components of a generalized icy body. This model consists of an undifferentiated iron/silicate core that produces heat through radioactive decay, subsurface ocean, time evolving clathrates, a water ice shell that can generate heat through tidal dissipation, and a thin surface layer of volatile ices.

Compositional Layers: The core is assumed to be a homogeneous mixture of iron and silicate material with a density of 3360 kg/m^3 and is treated as fully conductive. The subsurface ocean, when present, is assumed to convect on timescales much shorter than the timesteps used in the model (~100 ka). The ocean is therefore modelled as instantaneously transporting heat from the top of the core to the base of the ice shell, and changes thickness over time to keep the base of the ice shell at its melting point, while considering the storage and release of latent heat.

We additionally follow Carnahan et al. (2022) in proscribing the characteristics of a mixed clathrate and water ice shell as a function of clathrate percentage. Total ice shell thickness varies with time as a function of ocean temperature, pressure, and composition. The ice layer is divided into convective and conductive portions using a flux balance across the viscous layer. The volatile layer at the surface is assumed to be conductive, with thermal conductivity lower than that of water ice, and to be in vapor pressure equilibrium with a tenuous atmosphere.

Constitutive Equations: The governing equation for our model is the radially symmetric (1D) thermal diffusion equation in spherical coordinates:

$$\rho c_p \frac{dT}{dt} = \frac{1}{r^2}\frac{d}{dr}\left(k(T) r^2 \frac{dT}{dr}\right) + q(r,t),$$

where ρ is the material density, c_p is the specific heat capacity, k is the thermal conductivity which varies as a function of temperature, and q is a volumetric power density source term that varies in both space and time.

The upper portion of the ice shell is treated as a fully elastic material, with a thickness determined by the surface temperature, reference viscosity of ice, and model timestep. Heat transfer in this layer occurs solely through diffusion. The lower portion of the ice shell is treated as a viscous material on timescales comparable to the model timestep. The largest creep viscosity considered here is: $\eta_{max} = \Delta t \cdot E$, where E is the shear modulus of ice and Δt is the model timestep. Ice with a viscosity higher than η_{max} is treated as a fully elastic material.

Convection is approximated with scaling laws similar to those described by Deschamps and Sotin (2001); conductive heat flux is multiplied by the Nusselt number: $Nu = a\theta^{-4/3} Ra^{1/3}$, where Ra is the Rayleigh number and θ is a factor accounting for the viscosity contrast across this portion of the ice shell. Convection occurs when $Nu \geq 1$; otherwise, heat is transported through the viscous layer via diffusion.

For simplicity, and due to broad uncertainties in its rheology, viscous ice is assumed to behave as a fully Newtonian material. Its viscosity varies with temperature as:

$$\eta(T) = \eta_m exp\left[\frac{Q}{R}\left(\frac{1}{T} - \frac{1}{T_m}\right)\right],$$

where T_m is the melting point of the water ice and η_m is the reference viscosity at the melting temperature.

A flux balance is used at the surface of the body to allow for time-variable surface temperatures:

$$\sigma T_{surf}^4 = F_{cond} + (1 - a)\sigma T_{eq}^4,$$

where σ is the Stefan-Boltzmann constant, F_{cond} is the conductive heat flux from the interior, a is the Bond albedo, and T_{eq} is the equilibrium surface temperature for a given solar luminosity and planetary semimajor axis. We plan to implement the sublimation of volatile ices at the surface, which can be a significant sink of surface energy at temperatures above ~100 – 120 K.

Preliminary Results: Results were produced for the simple test cases of a pure water ice shell and a shell capped by a uniform thickness of nitrogen ice. In both cases, a subsurface ocean forms rapidly and achieves a maximum thickness after around 1 Ga, while the core reaches its maximum temperature of ~1200 K after around 2.5 Ga.

Acknowledgements: This work was performed at the Jet Propulsion Laboratory, California Institute of Technology, under contract with the National Aeronautics and Space Administration through the Solar System Workings program, grant #80NM0018F0612.

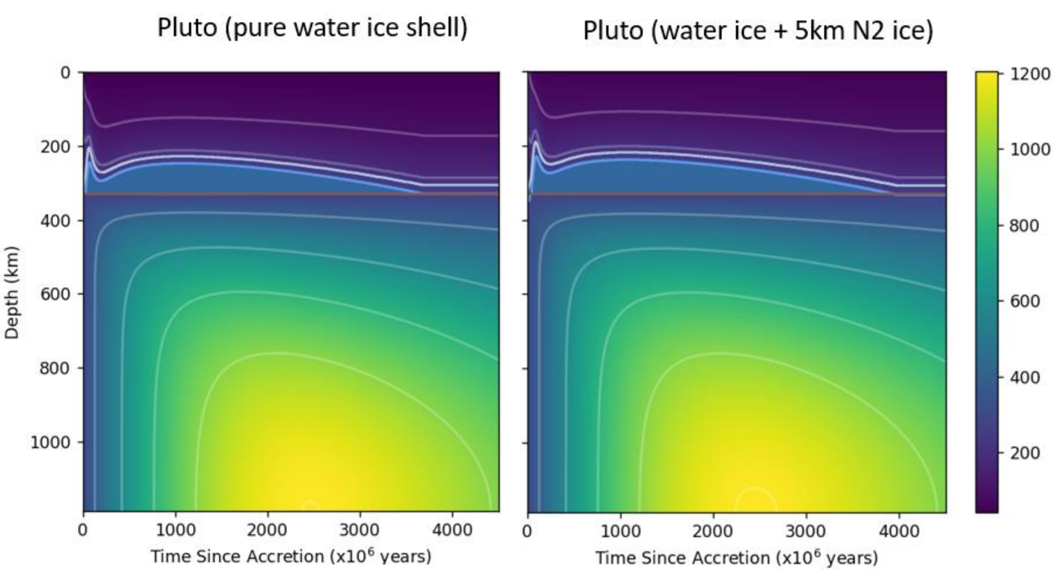

Figure 2: Preliminary model results for the thermal evolution of Pluto's interior for two simple cases. The brown line is at the top of the core, and the light blue shaded area shows ocean thickness over time. The ocean lasts ~.3 Ga with the nitrogen cap.

References: [1] McKinnon (1984). *Nature* **311**, 355-258. [2] McKinnon and Kirk (2014). [3] Grundy and Young (2004). *Icarus* **172**, 455–465. [4] Moore et al. (2016). *Science* **351**, 1284-1293. [5] McKinnon et al. 2016. *Nature* **534**, 82–85. [6] Grundy et al. (2016). *Science* **351**, 1283-1294. [7] Ahrens et al. (2021). *Geosciences* **12**. [8] Tobie et al. (2005). *Icarus* **175**, 496–502. [9] Desch et al. (2009). *Icarus* **202**, 694–714. [10] Robuchon and Nimmo (2011). *Icarus* **216**, 426-439. [11] Nimmo and Spencer (2015). *Icarus* **246**, 2-10. [12] Vance et al. (2018), *JGR: Planets* **123**, 180–205. [13] Carnahan et al. (2022). *GRL* **49**. [14] Deschamps and Sotin (2001). *JGR* **106**, 5107-5121.